Scientia Iranica, Vol. 10, No. 2, pp 164–174

SCIENTIA
IRANICA

Modeling Spatial Variability of Daily Rainfall in Southwest Iran

B. Saghafian[1], M. Tajrishy*, H. Taheri Shahraini[2] and N. Jalali[1]

Rainfall characteristics, which include spatial variability, exert a major influence on runoff properties. Many techniques have been proposed for determining the spatial distribution of daily rainfall. One of these techniques is spatial modeling, based on rainfall data measured by rain-gauge networks. In this study, application of different interpolation methods in the GIS environment, for estimating the spatial distribution of daily rainfall in the southwest of Iran with low rain-gauge density, have been compared on a regional scale. The cross validation technique was selected as an accuracy index and statistical parameters, such as MAE (Mean Absolute Error) and MBE (Mean Bias Error), were used for comparing the results of cross validation. The ranking of MAE and MBE values was used for determining the best interpolation method. The interpolation methods that were studied for mapping the spatial distribution of daily rainfall include nearest point, moving average, moving surface, trend surface and kriging. Since the spatial pattern of daily rainfall is random, the moving average method, with inverse distance weight function, was determined as the best method for interpolating daily rainfall data in the region of study.

INTRODUCTION

Meteorological and hydrological studies must be conducted as part of any water resources planning projects. Determining the runoff quantity from catchments is a rather complex task, which has become increasingly important for hydrologists over the last decades. Rainfall characteristics, including its spatial distribution, exert a major influence on runoff properties. The shape, timing and peak of a stream flow hydrograph are affected by spatial and temporal variability in rainfall [1]. The spatial distribution of rainfall is also important for the design of modern data acquisition systems and the modeling of rainfall [2].

Many techniques have been proposed for determining the spatial distribution of rainfall. One of these techniques is rainfall mapping by satellite-based data [2]. Rainfall estimates from satellite-based data are widely used in global climatological studies because they cover large areas, specially in regions with no traditional rainfall observation systems such as ground-based radar or rain-gauges [3].

Traditional techniques of modeling rainfall spatial distribution relies on rainfall data measured by rain-gauges. The importance of the rainfall spatial model has been acknowledged by Bevan and Hornberger [4], who stated that accurate portrayal of spatial variation in rainfall is a prerequisite for accurate simulation of stream flows. Similar conclusions were drawn earlier by Dawdy and Bergmann [5] and Wilson et al. [6]. Despite the recognized importance of the model for describing the spatial distribution of rainfall, little work has been undertaken on the use of new techniques [7]. Most of the models commonly used for estimation of spatial distribution of rainfall were developed prior to the advent of digital computers and the subsequent development of hydroinformatic tools, such as Geographic Information Systems (GIS). Recent developments in information sources have also enabled assessment of errors introduced through the use of alternative models for estimating the spatial variability of rainfall [7].

Several interpolation methods were applied by Dirks et al. [8] on hourly, daily, monthly and annual rainfall data from a dense network of 13 rain-gauges

1. *Soil Conservation and Watershed Management Research Institute, Ministry of Jihad Agriculture, Tehran, I.R. Iran.*
*. *Corresponding Author, Department of Civil Engineering, Sharif University of Technology, Tehran, I.R. Iran.*
2. *Department of Civil Engineering, Sharif University of Technology, Tehran, I.R. Iran.*

on Norfolk Island in the South Pacific (area 35 km^2). The results showed that the most computational demanding method, i.e. kriging, provided no significant improvement over much simpler inverse-distance or Thiessen methods, while the inverse-distance method was identified as the best method for interpolation of spatially dense rain-gauge networks for hourly or greater-times rainfall [8]. Seo [9] compared two procedures involving two different states of kriging for estimation of an hourly rainfall amount using hourly rain-gauge data from the operational network in Tulsa, Oklahoma. Sen [10] suggested that a Percentage Weighting (PW) method is more reliable and flexible than Thiessen polygon procedure for modeling the spatial distribution of rainfall. Borga and Vizzaccaro [11] compared kriging and multiquadratic surface fitting methods for estimating the hourly rainfall of real storm events. The results showed that kriging performed better at lower gauge density while, at higher gauge density, the accuracy of both estimators were similar [11]. Amani and Lebel [12] determined rainfields by interpolation with classic two-dimensional algorithms such as kriging and moving average.

Ball et al. [7] estimated the rainfall intensity in real and artificial storms by Thiessen polygons, inverse-distance, kriging, polynomial surfaces and spline surface methods in a 112 km^2 catchment in Australia. They concluded that spline surface was the most accurate estimator and Thiessen polygons provided the worst prediction [7]. Abtew et al. [13] showed that the kriging method was the appropriate method for determining the spatial distribution of monthly rainfall in South Florida, U.S.A. [13]. Kriging, moving average and spline surface methods were compared for annual rainfall mapping in the central basin of Iran. The results of cross validation showed that the spline surface, followed by the kriging method, was the most accurate method, while the moving average method was not appropriate for estimating annual rainfall [14].

According to the literature, interpolation methods are widely used for estimating the spatial distribution of annual and monthly rainfall. Yet, there are a few studies reported on modeling the spatial distribution of daily rainfall. In this study, application of different interpolation methods for estimating the spatial distribution of daily rainfall in the southwest region of Iran are compared in the GIS environment. Cross validation technique has been selected as the accuracy index. The motivation behind this work has been the need to estimate the spatial distribution of black rain which occured in the region due to the burning of Kuwaiti oil wells in 1991. Thus, the study is conducted on a regional basis covering several river basins. In the next section, interpolation methods implemented within the ILWIS GIS [15] are described.

ALTERNATIVE INTERPOLATION METHODS

Several land management activities require the spatially continuous estimation of environmental parameters, such as temperature, rainfall and radiation, etc. which are usually measured locally. Various interpolation methods have been applied for this purpose [16]. The most common interpolation methods used for mapping spatial distribution of point rainfall are nearest point, moving average, moving surface, trend surface and kriging. These methods are provided by a large number of GIS software, such as that used in this study: ILWIS [15]. A brief description of each of these methods is outlined as follows.

Nearest Point

The nearest point operation is also known as the nearest neighbor or Thiessen polygon [15]. The Thiessen method is probably the most common approach in modeling the spatial distribution of rainfall. This method was first proposed by Thiessen [17]. The approach is based on defining the area closer to a given gauge than any alternate gauge and the assumption that the best estimate of rainfall on that area is represented by the point measurement at the closest gauge. Since the basis of this model is the geometry of the region and gauge locations, implementation of Thiessen polygon in a GIS is straightforward [7]. In context of a raster GIS, the nearest point operation requires the point map of rain-gauges as input and the raster map of rainfall distribution is returned as output [15]. Each pixel in the output map is assigned the class, name, identifier or value of the nearest point [15].

Moving Average

The main disadvantage of the Thiessen interpolation method is the loss of rainfall spatial gradient. To overcome this problem, other methods have been developed that incorporate the spatial gradient of rainfall [8]. The moving average method accounts for the spatial gradient of rainfall by performing a weighted averaging on point values based on a weight function, an exponent and a limiting distance [18]. Two weight functions expressed by the following relations are available; inverse distance (w_1) and linear decrease (w_2) [15]:

$$w_1 = (1/d^{n'}) - 1, \quad (1)$$

$$w_2 = 1 - d^{n'}, \quad (2)$$

where n' is the weight exponent and d is the relative distance of a point to output pixel (D/D_0), in which D is the euclidean distance of the point to output pixel and D_0 is the limiting distance.

Note that the weight values decrease with increasing distance. The inverse distance weighted method, as presented by Watson and Philip (1985), estimates the rainfall at a point by a weighted interpolation, based on the distance of each rainfall gauge from the point where the rainfall estimate is required [18]. The typical values for the exponent in an inverse distance method are in the range of 0.5 to 3 [7]. The inverse distance function may be selected when accurately measured point data are available. On the other hand, the linear decrease function is suitable for point maps where measurement errors exist and points lying close to each other hold different values [15]. Similar to the Thiessen method, the inverse-distance weights are based on the region geometry and, hence, can be implemented easily in any raster GIS.

For each output pixel, the rainfall value is calculated as the sum of the products of the calculated weights and point rainfall values, divided by the sum of weights.

$$Z = \sum_{i=1}^{n}(w_i \times Z_i) / \sum_{i=1}^{n} w_i, \tag{3}$$

where w_i is the weight value for gauge i, Z_i is the rainfall value at gauge i, Z is the rainfall value for any output pixel and n is the total number of point rain-gauges.

Moving Surface

In this method, weight factors should be calculated by the method described in the previous section. Then, weight factors and rainfall values are multiplied, where the results of multiplication are known as weighted rainfall values. The rainfall value at any point may be calculated by fitting a polynomial surface through all of the weighted rainfall values of rainfall measurements which fall within the limiting distance [15]. The best polynomial surface should have the minimum square error. The polynomial surface may be expressed by:

$$f(x,y) = \sum b_{tu} x^t y^u, \tag{4}$$

where b_{tu} is a coefficient, x and y are coordinates, t and u are exponents, and $f(x,y)$ is the estimated rainfall value at (x,y) location. The summation of t and u determines the degree of polynomial surface. For example, the 2nd-degree linear surface formula can be written as:

$$f(x,y) = b_{10}x + b_{11}xy + b_{01}y + b_{00}. \tag{5}$$

The moving surface operation in a raster GIS requires a point map as the input map and returns a raster map as the output.

Polynomial (Trend) Surface

Polynomial surfaces are based on constructing a surface to fit the input point data with least-square minimization of the errors [7]. The form of polynomial function follows Equation 4, where the coefficients (b_{tu}) are chosen to minimize the following function:

$$E = \sum_{i=1}^{n}[p(x_i,y_i) - f(x_i,y_i)]^2, \tag{6}$$

where n is the number of rain-gauges, $p(x_i,y_i)$ is the observed value of rainfall at gauge i, $f(x_i,y_i)$ is the estimated rainfall at gauge i and E is the error function to be minimized.

Kriging

Although the inverse-distance method shows the spatial trends in rainfall, it is limited in that the exponent of weighting functions needs to be preselected. The choice of exponent may significantly affect the resulting interpolated field [8]. The method of kriging avoids the need to preselect the parameters [8]. Kriging is based on extracting semivariogram from the input point map. The semivariogram formula can be written as:

$$\gamma = \frac{\sum_{i=1}^{n}\sum_{j=1}^{n} w_{ij}(Z_i - Z_j)}{2\sum_{i=1}^{n}\sum_{j=1}^{n} w_{ij}}, \tag{7}$$

where w_{ij} is the weight of a pair of points i and j, Z_i and Z_j are input values at i and j, respectively and γ is the semivariogram. When a pair of points (i,j) belongs to a certain distance class, then $w_{ij} = 1$, otherwise $w_{ij} = 0$. If the semivariogram formula is calculated for several points of an input point map, the following matrix can be constructed:

$$[r] = \begin{bmatrix} 0 & \gamma(h_{12}) & \cdots & \gamma(h_{1n}) & 1 \\ \gamma(h_{21}) & 0 & \cdots & \gamma(h_{2n}) & 1 \\ \cdots & \cdots & \cdots & \cdots & \cdots \\ \gamma(h_{n1}) & \gamma(h_{n2}) & \cdots & 0 & 1 \\ 1 & 1 & \cdots & 1 & 0 \end{bmatrix}, \tag{8}$$

where h_{ij} is the distance between the input points i and j and γ is the value of the semivariogram model corresponding to the distance h_{ij}.

The semivariogram model must be known from the semivariogram values and several models have been proposed to fit them. Two major groups of semivariogram models are stationary and non-stationary.

The stationary models (such as spherical, gaussian, circular and exponential) have a sill value. Sill is the semivariogram model value when the semivariogram model is equal to the variance of the measured point values [18]. For example, a spherical model may be expressed by:

$$\gamma(h) = C_0 + C \times \left[\frac{3h}{2a} - \frac{h^3}{2a^3}\right], \quad \text{for} \quad 0 < h < a,$$
$$\gamma(h) = C_0 + C, \quad \text{for} \quad h \geq a, \tag{9}$$

where a is the range of the semivariogram model, h is the distance, C_0 is the nugget effect, C is the difference between the sill and nugget effect and $\gamma(h)$ is the value of the semivariogram model for distance h. Figure 1 shows a schematic view of a stationary semivariogram model.

A semivariogram with a nugget effect does not pass the origin. The variables of semivariogram values are normally erratic over the short distances where the semivariogram increases from zero to the level of the nugget effect, in a distance less than the sampling distance [15]. However, non-stationary models (such as linear and power models) don't have any sill value. For example, the power model may be expressed by:

$$\gamma(h) = C_0 + sh^p, \quad \text{for} \quad 0 \leq p \leq 2, \tag{10}$$

where p is the exponent value of the model, s is the slope value of the model, C_0 is the nugget effect value and $\gamma(h)$ is the value of the semivariogram model for distance h.

Now, the following matrix may be determined:

$$[D'] = \begin{bmatrix} \gamma(h_{o1}) \\ \gamma(h_{o2}) \\ \vdots \\ \gamma(h_{on}) \\ 1 \end{bmatrix}, \tag{11}$$

where h_{oi} is the distance between the output pixel and input point i and $\gamma(h_{oi})$ is the value of the semivariogram model for distance h_{oi}. The kriging weight factors may be found by solving this matrix equation:

$$[r] \times [w] = [D']. \tag{12}$$

The summation of weight factors (w_i) in $[w]$ for different point values matrix should be unity. The estimated output pixel value can be calculated by:

$$Z = \sum_{i=1}^{n} (w_i \times Z_i). \tag{13}$$

This algorithm should be performed for all output pixels [15].

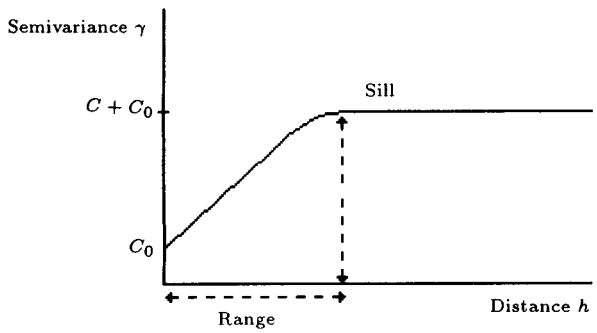

Figure 1. Schematic view of the stationary semivariogram model.

EVALUATION CRITERIA

The cross validation (or fictitious-point method) technique is used in this study for evaluating different interpolation methods. This criteria was first proposed by Seaman [19], where the real value at one point, or at a number of points, is removed from the data set and interpolation is performed on the remaining points. Then the estimated values of the removed points are compared with the real values using statistical parameters. In this study, Mean Absolute Error (MAE) and Mean Bias Error (MBE) are used for the evaluation of errors corresponding to different methods. MAE and MBE are calculated by the following equations:

$$\text{MAE} = \frac{\sum_{i=1}^{n} |Z_{ei} - Z_{ri}|}{n}, \tag{14}$$

$$\text{MBE} = \frac{\sum_{i=1}^{n} (Z_{ei} - Z_{ri})}{n}, \tag{15}$$

where Z_{ei} and Z_{ri} are the estimated and real values of rainfall at point i, respectively.

REGION OF STUDY

The study region is located in the southwest of Iran, north of the Persian Gulf. The region boundaries are (46° to 57°, 24′)E and (26° to 33°, 24′)N. Figure 2 shows the DEM and location of the study region in Iran. The area of study region is approximately 590,000 km^2 with 46 reliable synoptic and climatological gauges (Figure 3). Two rainfall events of March 7, 1991 and February 21, 1991, which roughly covered the entire region, are studied. Figure 3 shows the depth of daily rainfall in milimeters for March 7, 1991. The positive signs show the location of gauges. The rainfall data has been provided by the Meterological Organization of Iran.

Because of the high spatial changes in the climate conditions and elevations in the study region, the daily rainfall shows high spatial variations.

Table 1. MAE values corresponding to different polynomial (trend) surface methods.

	Plane	2nd Degree Linear	2nd Degree Parabolic	2nd Degree	3rd Degree
5 Points Removed	9.0	7.6	7.8	6.8	7.0
5 Points Removed	9.9	8.1	9.4	8.3	30.4
10 Points Removed	8.0	10.2	10.7	11	12.6
12 Points Removed	6.9	7.5	7.1	7.9	13.0
15 Points Removed	8.0	8.0	7.5	8.9	9.4

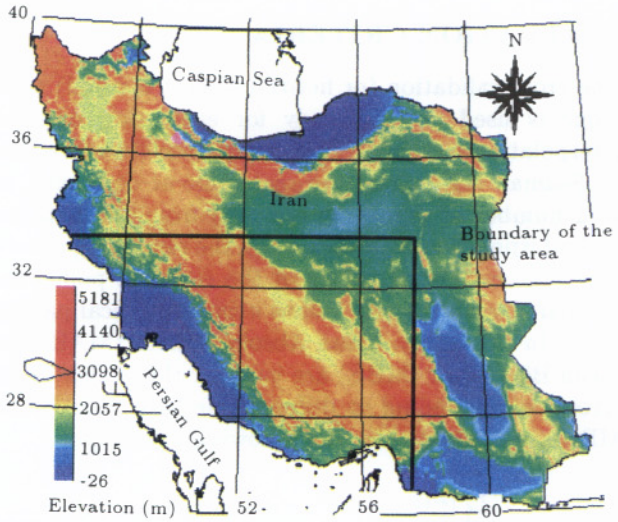

Figure 2. DEM and location of the study region in Iran.

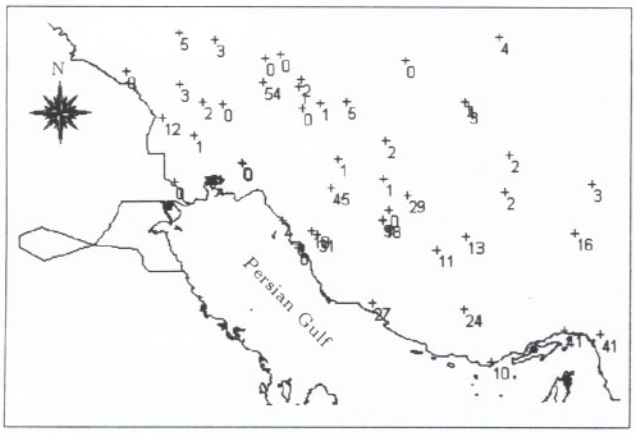

Figure 3. Location of the rain-gauges (positive signs) and the amount of rainfall (mm) observed on March 7, 1991.

RESULTS

Suitable Option for Each Interpolation Methods

Due to the variety of options available in each interpolation technique, it is first necessary to choose the most suitable option associated with different methods. Cross validation was performed by randomly removing sets of 5, 10, 12 and 15 points from the original rainfall point map of March 7, 1991. Consequently, several new point interpolated maps are produced each time.

Different polynomial surface methods, such as plane, second degree linear, second degree parabolic ($f(x,y) = a + bx + cy + dx^2 + ey^2$), second degree ($f(x,y) = a + bx + cy + dx^2 + ey^2 + fxy$) and third degree, were performed to produce interpolated rainfall maps. Figure 4 shows rainfall distribution in the study region produced by the second degree linear polynomial (trend) surface method, where negative values imply the inability of this method to predict daily rainfall. The best method was determined by calculating the corresponding MAE and MBE values. Tables 1 and 2 show the MAE and MBE values in different rain-gauge removing states. Table 3 summarizes the sum of accuracy ranks in Tables 1 and 2. The ranking method assigns rank numbers from 1 to m (m being the number of compared different methods) to different method on the basis of the amount of error values. For example, the ranking values of 1 to 5 are assigned to five MAE values in each row of Table 1 and then the summation of ranking values in each column should be computed for determining the sum of MAE ranks. The ranking

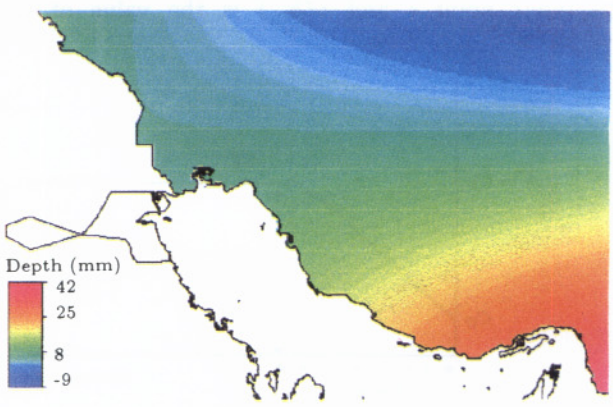

Figure 4. Interpolated rainfall map based on the trend surface (2nd degree linear) method.

Table 1. MAE values corresponding to different polynomial (trend) surface methods.

	Plane	2nd Degree Linear	2nd Degree Parabolic	2nd Degree	3rd Degree
5 Points Removed	9.0	7.6	7.8	6.8	7.0
5 Points Removed	9.9	8.1	9.4	8.3	30.4
10 Points Removed	8.0	10.2	10.7	11	12.6
12 Points Removed	6.9	7.5	7.1	7.9	13.0
15 Points Removed	8.0	8.0	7.5	8.9	9.4

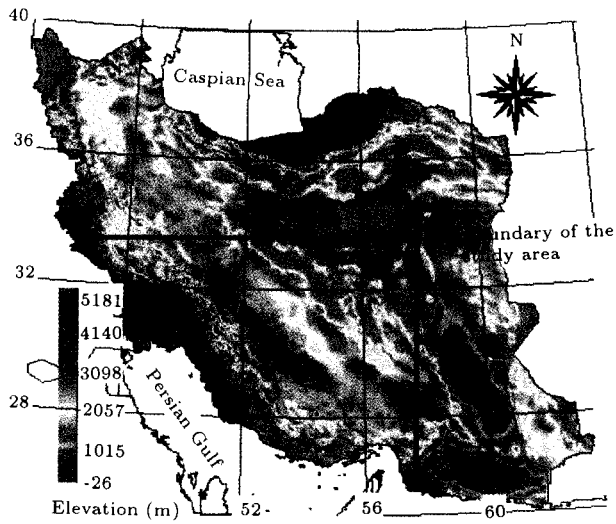

Figure 2. DEM and location of the study region in Iran.

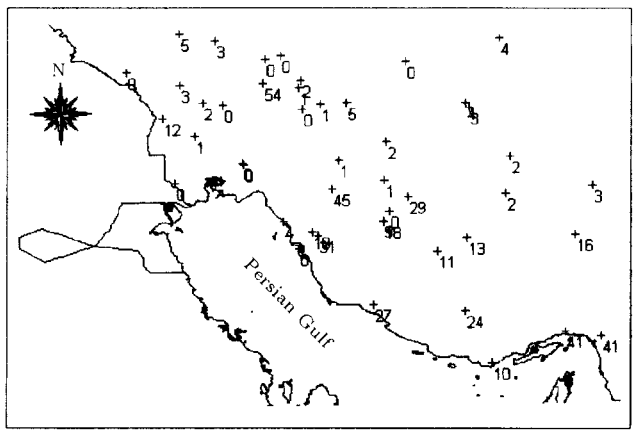

Figure 3. Location of the rain-gauges (positive signs) and the amount of rainfall (mm) observed on March 7, 1991.

RESULTS

Suitable Option for Each Interpolation Methods

Due to the variety of options available in each interpolation technique, it is first necessary to choose the most suitable option associated with different methods. Cross validation was performed by randomly removing sets of 5, 10, 12 and 15 points from the original rainfall point map of March 7, 1991. Consequently, several new point interpolated maps are produced each time.

Different polynomial surface methods, such as plane, second degree linear, second degree parabolic ($f(x,y) = a + bx + cy + dx^2 + ey^2$), second degree ($f(x,y) = a + bx + cy + dx^2 + ey^2 + fxy$) and third degree, were performed to produce interpolated rainfall maps. Figure 4 shows rainfall distribution in the study region produced by the second degree linear polynomial (trend) surface method, where negative values imply the inability of this method to predict daily rainfall. The best method was determined by calculating the corresponding MAE and MBE values. Tables 1 and 2 show the MAE and MBE values in different rain-gauge removing states. Table 3 summarizes the sum of accuracy ranks in Tables 1 and 2. The ranking method assigns rank numbers from 1 to m (m being the number of compared different methods) to different method on the basis of the amount of error values. For example, the ranking values of 1 to 5 are assigned to five MAE values in each row of Table 1 and then the summation of ranking values in each column should be computed for determining the sum of MAE ranks. The ranking

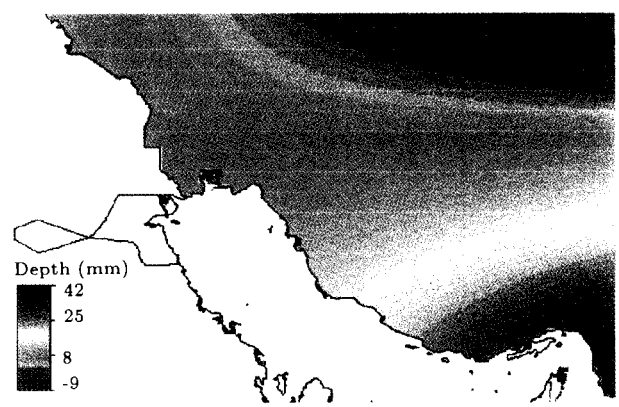

Figure 4. Interpolated rainfall map based on the trend surface (2nd degree linear) method.

Table 2. MBE values corresponding to different polynomial (trend) surface methods.

	Plane	2nd Degree Linear	2nd Degree Parabolic	2nd Degree	3rd Degree
5 Points Removed	9.0	7.6	7.8	7.0	-2.0
5 Points Removed	-6.3	-5.4	-7.5	-6.5	-6.7
10 Points Removed	3.0	3.4	5.7	2.5	2.7
12 Points Removed	5.8	6.0	7.4	3.9	11.1
15 Points Removed	2.5	1.3	1.1	2.9	4.9

Table 3. Sum of accuracy ranks of different trend surface methods.

	Plane	2nd Degree Linear	2nd Degree Parabolic	2nd Degree	3rd Degree
Sum of MAE Ranks	13	11	13	15	22
Sum of MBE Ranks	15	13	19	11	17
Sum of MAE and MBE Ranks	28	24	32	26	39

values in Table 3 imply that second degree linear is the best method.

The results of applying a moving average (inverse-distance) with exponent values of 2 and 3 are compared after randomly removing 5, 10, 12 and 15 points from the original rainfall map. Tables 4 and 5 show cross validation results for different randomly removing point states. Table 6 shows the sum of accuracy ranks of the MAE and MBE values. The results show that the exponent 3 has performed better than that of exponent 2. Figure 5 represents rainfall distribution in the study region produced by inverse distance method with exponent 3.

The moving surface method is examined with exponent 3 of the inverse distance in second degree linear and third degree surface methods, with removal of 10 and 15 points. After interpolation and calculation of MAE and MBE for each method, it is found that second degree linear performs better than third degree surface. Values of MAE and MBE for each method are presented and compared in Tables 7 and 8. Figure 6 shows rainfall distribution in the study region produced by a moving surface with exponent 3 with

Table 4. MAE values corresponding to inverse distance method with exponent 2 and 3.

	$n = 2$	$n = 3$
5 Points Removed	4.2	3.5
10 Points Removed	8.6	8.3
12 Points Removed	6.4	6.5
15 Points Removed	8.7	9.1

Table 5. MBE values corresponding to inverse distance method with exponent 2 and 3.

	$n' = 2$	$n' = 3$
5 Points Removed	4.2	3.5
10 Points Removed	3.9	3.4
12 Points Removed	5.2	5.1
15 Points Removed	4.4	4.9

Table 6. Sum of accuracy ranks for inverse distance methods.

	$n' = 2$	$n' = 3$
Sum of MAE Ranks	6	6
Sum of MBE Ranks	7	5
Sum of MAE and MBE Ranks	13	11

Table 7. MAE values corresponding to moving surface method with 2nd-degree linear and 3rd-degree surface.

	2nd Degree Linear	3rd Degree
10 Points Removed	10.5	11.1
15 Points Removed	8.5	16.1

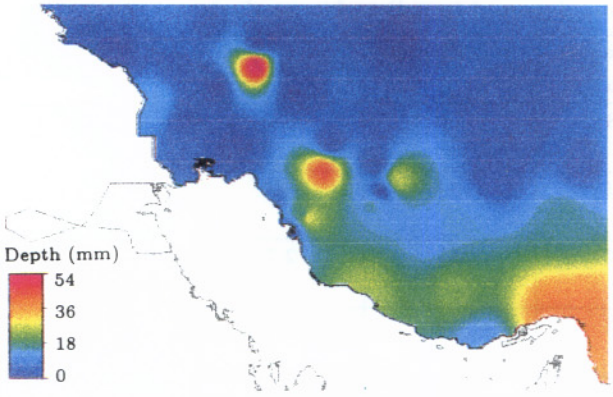

Figure 5. Interpolated rainfall map based on the inverse distance method with exponent 3.

Table 8. MBE values corresponding to moving surface method with 2nd-degree linear and 3rd-degree surface.

	2nd Degree Linear	3rd Degree
10 Points Removed	0.0	8.2
15 Points Removed	4.2	11.8

inverse distance and second degree linear surface.

Prior to the application of the kriging method, the semivariogram model must be determined. The empirical semivariogram data of the March 7 rainfall event is similar to the stationary semivariogram pattern in the initial part of the semivariogram (Figure 7). But the overall semivariogram resembles a non-stationary semivariogram pattern (Figure 8). This implies that daily rainfall has a non-stationary random pattern. However, the semivariogram showed high variability and didn't follow any of the known models. Various stationary and non-stationary models were fitted to the data to determine the best model. Spherical, circular, exponential and gaussian stationary models were examined in Figure 7. The semivariogram characteristics of the models were estimated as: sill = 190, nugget effect = 30 and range = 3.

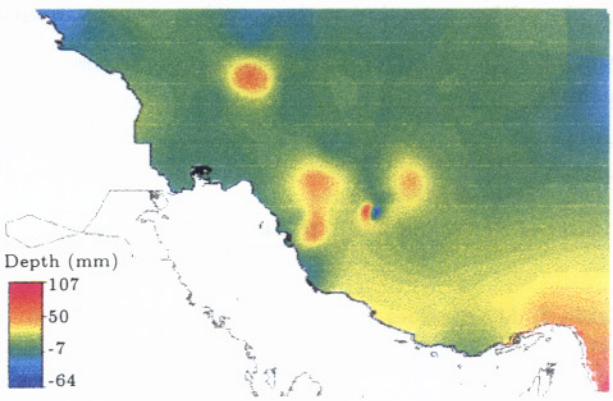

Figure 6. Interpolated rainfall map based on the 2nd degree linear moving surface (inverse distance) method with exponent 3.

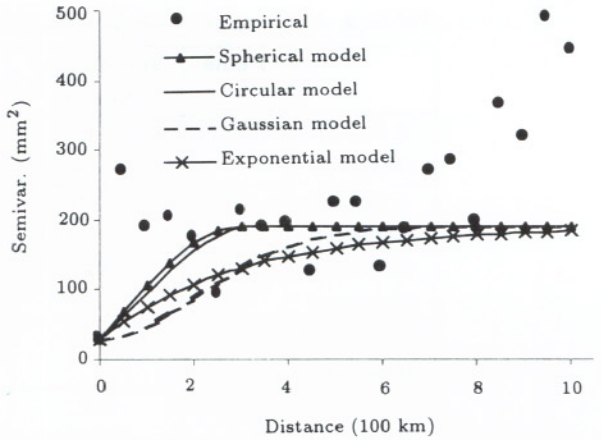

Figure 7. Empirical semivariogram data and different stationary semivariogram model.

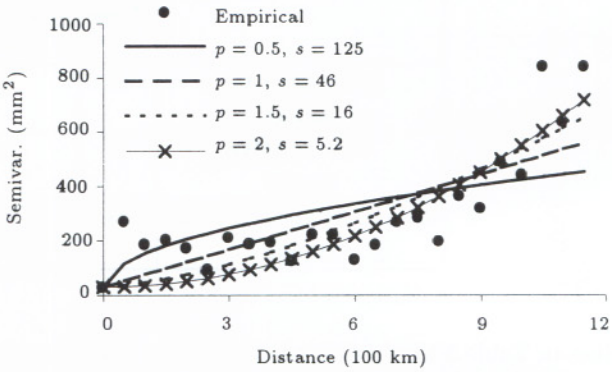

Figure 8. Empirical semivariogram data and different non-stationary semivariogram model.

The Root Mean Square Error (RMSE) values of different models are shown in Table 9, where the spherical model stands as the best stationary model. Therefore, the kriging method with the spherical model was chosen for comparison with other interpolation methods. Figure 9 represents the rainfall distribution in the study region for March 7, 1991, produced by the kriging method with an assumed spherical semivariogram model.

As for the non-stationary model, power models with different exponent values were fitted to the empirical semivariogram values (Figure 8). The RMSE values of different power models are shown in Table 10, where a power model with an exponent equal to two is the best non-stationary power model. The kriging method

Table 9. RMSE values for different stationary models.

	Spherical Model	Circular Model	Gaussian Model	Exponential Model
RMSE	48.0	48.1	48.9	49.0

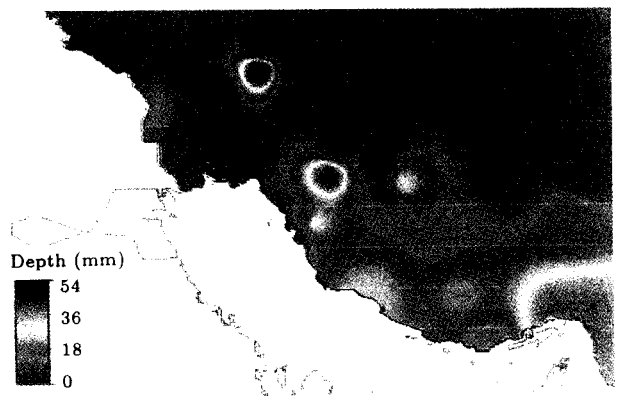

Figure 5. Interpolated rainfall map based on the inverse distance method with exponent 3.

Table 8. MBE values corresponding to moving surface method with 2nd-degree linear and 3rd-degree surface.

	2nd Degree Linear	3rd Degree
10 Points Removed	0.0	8.2
15 Points Removed	4.2	11.8

inverse distance and second degree linear surface.

Prior to the application of the kriging method, the semivariogram model must be determined. The empirical semivariogram data of the March 7 rainfall event is similar to the stationary semivariogram pattern in the initial part of the semivariogram (Figure 7). But the overall semivariogram resembles a non-stationary semivariogram pattern (Figure 8). This implies that daily rainfall has a non-stationary random pattern. However, the semivariogram showed high variability and didn't follow any of the known models. Various stationary and non-stationary models were fitted to the data to determine the best model. Spherical, circular, exponential and gaussian stationary models were examined in Figure 7. The semivariogram characteristics of the models were estimated as: sill = 190, nugget effect = 30 and range = 3.

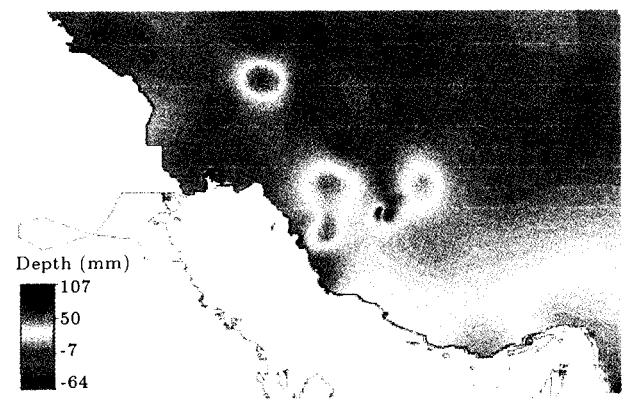

Figure 6. Interpolated rainfall map based on the 2nd degree linear moving surface (inverse distance) method with exponent 3.

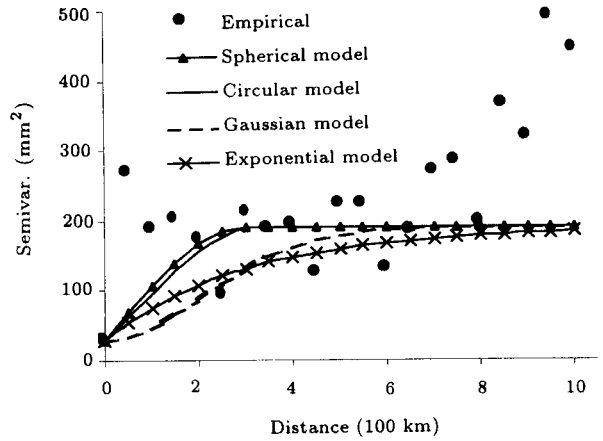

Figure 7. Empirical semivariogram data and different stationary semivariogram model.

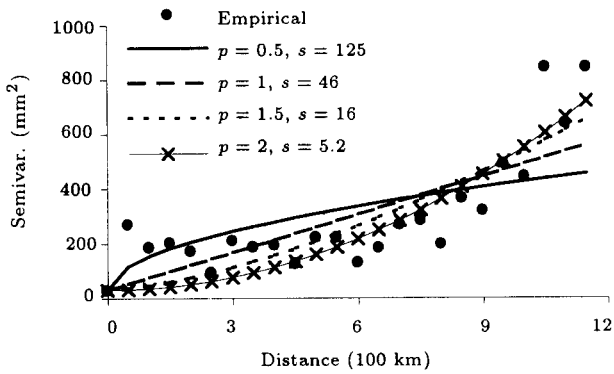

Figure 8. Empirical semivariogram data and different non-stationary semivariogram model.

The Root Mean Square Error (RMSE) values of different models are shown in Table 9, where the spherical model stands as the best stationary model. Therefore, the kriging method with the spherical model was chosen for comparison with other interpolation methods. Figure 9 represents the rainfall distribution in the study region for March 7, 1991, produced by the kriging method with an assumed spherical semivariogram model.

As for the non-stationary model, power models with different exponent values were fitted to the empirical semivariogram values (Figure 8). The RMSE values of different power models are shown in Table 10, where a power model with an exponent equal to two is the best non-stationary power model. The kriging method

Table 9. RMSE values for different stationary models.

	Spherical Model	Circular Model	Gaussian Model	Exponential Model
RMSE	48.0	48.1	48.9	49.0

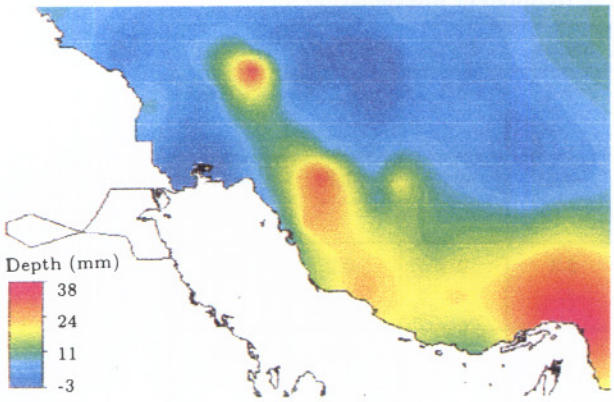

Figure 9. Interpolated rainfall map based on the kriging method with spherical semivariogram model.

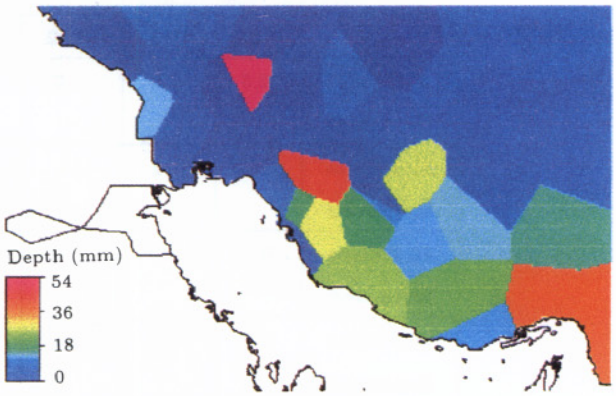

Figure 10. Interpolated rainfall map based on the Thiessen method.

Table 10. RMSE values for power model with different exponent values (p).

	$p = 0.5$	$p = 1.0$	$p = 1.5$	$p = 2.0$
RMSE	32.0	27.1	24.3	23.0

with this model was also selected for comparison with other interpolation methods.

Overall, the selected methods for further analysis consist of Thiessen (T), inverse distance with exponent 3 (ID3), moving surface (inverse distance) with second degree linear surface and exponent 3 (MS2), trend surface with second degree linear surface (TS2), kriging with spherical semivariogram model (KGsp), and kriging with power semivariogram model with exponent 2 (KGp2).

Determination of the Best Interpolation Method

In this section, the results of the application of all the selected methods in the previous section are computed. Random removal of 5 points from the rainfall point map in six scenarios, 10 points in four scenarios, 15 points in three scenarios and 20 points in two scenarios produces 15 new point maps. The interpolation operations were performed by Thiessen (Figure 10), i.e inverse-distance with exponent 3 (ID3), moving surface 2nd-degree linear with exponent 3 (MS2), MS2 method with converting the negative values to zero (MS2z), trend (polynomial) surface with 2nd-degree linear (TS2), TS2 with converting the negative values to zero (TS2z), kriging with spherical semivariogram model (KGsp) and power semivariogram model (KGp2) over the 15 new point maps. Due to the nature of mathematical relations used in the moving surface, polynomial surface and kriging (with spherical model) methods, negative values may be generated in the interpolated maps. Such negative values are converted to zero where found in the interpolated rainfall maps. The averages of MAE and MBE values corresponding to various point removal scenarios are calculated and reported in Tables 11 and 12.

Table 13 shows the sum of the accuracy ranks for different interpolation methods. According to Table 13, the inverse distance with exponent 3, followed by Thiessen, and MS2z clearly overweigh other methods for estimating the spatial distributions of daily rainfall. The results of the empirical semivariogram (Figure 8) and cross validation (Table 13) demonstrate that daily rainfall has random non-stationary distribution.

Table 11. Average values of MAE corresponding to different interpolation methods.

	T	ID3	MS2	TS2	MS2z	TS2z	KGsp	KGp2
5 Points Removed	8.5	8.1	9.9	9.6	8.4	9.3	9.3	9.6
10 Points Removed	7.8	8.0	9.0	9.3	8.2	9.0	9.1	9.3
15 Points Removed	8.1	7.9	8.2	8.7	7.9	8.3	8.9	8.9
20 Points Removed	7.7	7.6	9.2	9.4	7.7	9.0	8.6	9.6

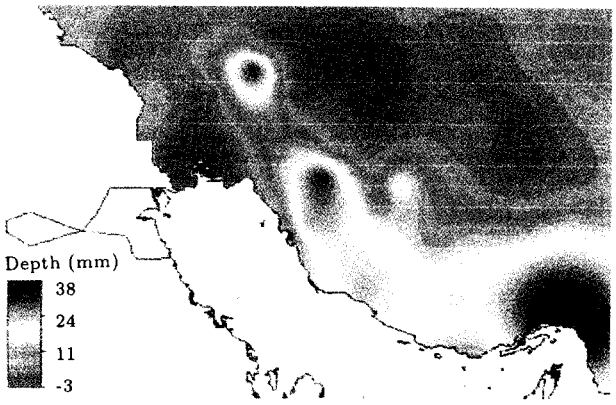

Figure 9. Interpolated rainfall map based on the kriging method with spherical semivariogram model.

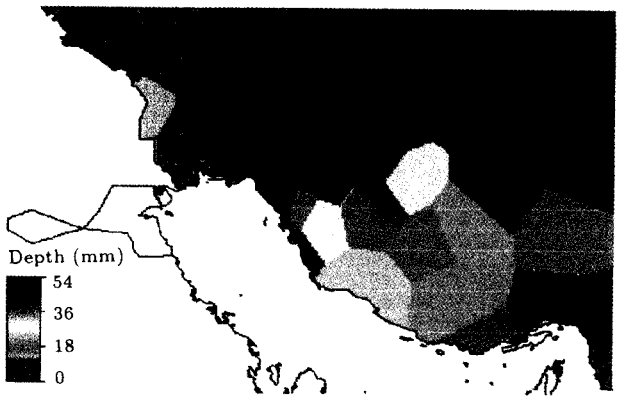

Figure 10. Interpolated rainfall map based on the Thiessen method.

Table 10. RMSE values for power model with different exponent values (p).

	$p = 0.5$	$p = 1.0$	$p = 1.5$	$p = 2.0$
RMSE	32.0	27.1	24.3	23.0

with this model was also selected for comparison with other interpolation methods.

Overall, the selected methods for further analysis consist of Thiessen (T), inverse distance with exponent 3 (ID3), moving surface (inverse distance) with second degree linear surface and exponent 3 (MS2), trend surface with second degree linear surface (TS2), kriging with spherical semivariogram model (KGsp), and kriging with power semivariogram model with exponent 2 (KGp2).

Determination of the Best Interpolation Method

In this section, the results of the application of all the selected methods in the previous section are computed. Random removal of 5 points from the rainfall point map in six scenarios, 10 points in four scenarios, 15 points in three scenarios and 20 points in two scenarios produces 15 new point maps. The interpolation operations were performed by Thiessen (Figure 10), i.e inverse-distance with exponent 3 (ID3), moving surface 2nd-degree linear with exponent 3 (MS2), MS2 method with converting the negative values to zero (MS2z), trend (polynomial) surface with 2nd-degree linear (TS2), TS2 with converting the negative values to zero (TS2z), kriging with spherical semivariogram model (KGsp) and power semivariogram model (KGp2) over the 15 new point maps. Due to the nature of mathematical relations used in the moving surface, polynomial surface and kriging (with spherical model) methods, negative values may be generated in the interpolated maps. Such negative values are converted to zero where found in the interpolated rainfall maps. The averages of MAE and MBE values corresponding to various point removal scenarios are calculated and reported in Tables 11 and 12.

Table 13 shows the sum of the accuracy ranks for different interpolation methods. According to Table 13, the inverse distance with exponent 3, followed by Thiessen, and MS2z clearly overweigh other methods for estimating the spatial distributions of daily rainfall. The results of the empirical semivariogram (Figure 8) and cross validation (Table 13) demonstrate that daily rainfall has random non-stationary distribution.

Table 11. Average values of MAE corresponding to different interpolation methods.

	T	ID3	MS2	TS2	MS2z	TS2z	KGsp	KGp2
5 Points Removed	8.5	8.1	9.9	9.6	8.4	9.3	9.3	9.6
10 Points Removed	7.8	8.0	9.0	9.3	8.2	9.0	9.1	9.3
15 Points Removed	8.1	7.9	8.2	8.7	7.9	8.3	8.9	8.9
20 Points Removed	7.7	7.6	9.2	9.4	7.7	9.0	8.6	9.6

Table 12. Average values of MBE corresponding to different interpolation methods.

	T	ID3	MS2	TS2	MS2z	TS2z	KGsp	KGp2
5 Points Removed	-2.5	-1.6	-3.0	-0.9	-2.4	4.3	3.1	-1.8
10 Points Removed	-2.3	-1.2	-3.1	-0.8	-2.3	-0.5	-1.7	-0.7
15 Points Removed	0.4	0.1	2.0	2.3	2.3	2.4	-0.2	-0.3
20 Points Removed	-2.3	-1.5	-4.0	-0.4	-2.5	-0.1	-2.2	-0.7

Table 13. Sum of accuracy ranks for different interpolation methods.

	T	ID3	MS2	TS2	MS2z	TS2z	KGsp	KGp2
Sum of MAE Ranks	8	5	22	26	8	18	21	28
Sum of MBE Ranks	21	11	27	12	23	18	19	11
Sum of MAE and MBE Ranks	29	16	49	38	31	36	40	39

Determination of the Best Interpolation Method in a Smaller Region

To examine the sensitivity of the results obtained for the entire region, similar interpolation operations were performed at a river basin scale bounded by (47°, 41′ to 51°,18′)E and (30°,10′ to 32°, 55′)N region. The area of this region is approximately 100,000 km^2, where a total of 12 gauges are located. Due to a limited number of gauges, a random removal of points was performed in six scenarios, each scenario involving the removal of only two gauges.

The interpolation methods were Thiessen, moving average (inverse-distance) with exponent 3, moving surface (inverse-distanse) with 2nd-degree linear and exponent 3 and trend surface with 2nd-degree linear surface. Negative values were transformed to zero in the two latter techniques. Kriging was not applied since none of the models fitted the semivariogram. This again demonstrates that there is non-stationary random distribution in daily rainfall values.

The results of ranking based on the accuracy reflected by average MAE and MBE values in six scenarios shown in Table 14, confirm the conclusion drawn for the entire region. Once again, the inverse distance is found as the most appropriate method for determining the spatial distribution of daily rainfall in a smaller region with higher gauge density.

Table 14. Sum of accuracy ranks of different interpolation methods in the subregion.

	T	ID3	MS2z	TS2z
Sum of MAE Ranks	13	12	17	16
Sum of MBE Ranks	13	13	18	16
Sum of MAE and MBE Ranks	26	25	35	32

Comparison of Kriging and Moving Average for Another Event

The comparison between kriging and moving average methods was performed on the study region for the rainfall event of February 21, 1991. The semivariogram was not similar to that of the previous rainfall event. A spherical model was fitted to the semivariogram. Random removal of points was performed in twenty five scenarios, where, in each scenario, only one gauge was removed. The results of cross validation are summarized in Table 15, where it shows that the inverse distance method may still be declared as the most suitable method for modeling the daily rainfall distribution.

The results of this study are in general agreement with those of Dirks et al. [8], although the two studies are quite different in the spatial scale of their region.

Table 15. Cross validation results for February 21, 1991 rainfall event.

	ID3	KGsp
MAE	8.1	7.2
MBE	2.9	3.5

They compared the Thiessen, mean area, inverse distance and kriging methods and concluded that the inverse distance method was the most appropriate choice for operational use over integration times of hourly or greater rainfall.

CONCLUSIONS

For this particular region under study, with very low rain-gauge density, the following conclusions were drawn:

1. Daily rainfall follows non-stationary random spatial distribution;
2. The inverse distance method with exponent 3 is the best method for interpolating daily rainfall, since the spatial pattern is non-stationary random and the inverse distance assumes no spatial trend;
3. The second best method for daily rainfall interpolation is the Thiessen method;
4. The methods which are based on existence of a spatial trend among points do not offer a suitable technique for daily rainfall interpolation;
5. The inverse distance method also outperforms other methods for a subregion of the study area with greater gauge density.

In general, the inverse distance method for modeling the spatial variability of daily rainfall on a regional scale with a low density rain-gauge produces more realistic rainfall fields and requires minor computational effort.

ACKNOWLEDGMENT

The authors would like to thank Peyman Arasteh, a member of the Soil Conservation and Watershed Management Research Center, for his review of the paper and Dr. B. Aminipouri for his partial support of the project. The data for this study has been provided by the Meteorological Organization of Iran.

NOMENCLATURE

a	range
b_{tu}	coefficient
C_0	nugget effect
C	difference between sill and nugget effect
D	euclidean distance of point to output pixel
D_0	limiting distance
d	relative distance of a point to output pixel
E	square error
$f(x_i, y_i)$	estimated rainfall at gauge i
h	distance
h_{ij}	distance between the input points i and j
h_{oi}	distance between the output pixel and input point i
MAE	Mean Absolute Error
MBE	Mean Bias Error
n	number of points or rainfall gauges or values
n'	weight exponent
p	exponent value of power model
$p(x_i, y_i)$	observed rainfall at gauge i
RMSE	Root Mean Square Error
s	slope of power model
t	exponent of x in polynomial surface
u	exponent of y in polynomial surface
w_i	weight value for point i
w_{ij}	weight of a pair point
x	longitude coordinate
y	latitude coordinate
Z	estimated value for output pixel
Z_i	value of input point i
Z_j	value of input point j
$[w]$	matrix of weight factors of points
γ	semivariogram
$\gamma(h_{ij})$	value of semivariogram model for distance h_{ij}
$\gamma(h_{oi})$	value of semivariogram model for distance h_{oi}

REFERENCES

1. Singh, V.P. "Effect of spatial and temporal variability in rainfall and watershed characteristics on stream flow hydrograph", *Hydrological Processes*, **11**(12), pp 1649-1669 (1997).
2. Da Serra Costa, F., Damazio, J.M., Das Neves, F.P. and Simabuguro, M.D. "Linking asynthetic storm generation model with IDRISI-GIS", *Application of Geographic Information Systems in Hydrology and Water Resources Management*, IAHS Publication, **235**, pp 107-113 (1996).
3. Mahani, S.E. and Sorooshian, S. "Application of remote sensing for hydrological purposes", *Proceedings of the*

First Regional Conference on Water Balance, Ahwaz, I.R. Iran, pp 93-104 (2000).

4. Bevan, K.J. and Hornberger, G.M. "Assessing the effect of spatial pattern of precipitation in modeling stream flow hydrographs", *Wat. Resour. Bull.*, **18**(5), pp 823-829 (1982).
5. Dawdy, D.R. and Bergmann, J.M. "Effect of rainfall variability on stream flow simulation", *Wat. Resour. Res.*, **5**, pp 958-966 (1969).
6. Wilson, C.B., Valdes, J.B. and Rodriguez-Irturbe, I. "On the influence of the spatial distribution of rainfall on storm runoff", *Wat. Resour. Res.*, **15**, pp 321-328 (1979).
7. Ball, J.E. and Luk, K.C. "Modeling spatial variability of rainfall over a catchment", *ASCE Journal of Hydrologic Engineering*, **3**(2), pp 122-130 (1998).
8. Dirks, K.N., Hay, J.E., Stow, C.D. and Harris, D. "High resolution studies of rainfall on Norfolk Island, Part II: Interpolation of rainfall data", *Journal of Hydrology*, **208**(3-4), pp 187-193 (1998).
9. Seo, D.J. "Real-time estimation of rainfall fields using rain gauge data under fractional coverage conditions", *Journal of Hydrology*, **208**(1-2), pp 25-36 (1998).
10. Sen, Z. "Average area precipitation by percentage weighted polygon method", *ASCE Journal of Hydrologic Engineering*, **3**(1), pp 69-72 (1998).
11. Borga, M. and Vizzaccaro, A. "On the interpolation of hydrologic variables: Formal equivalence of multiquadratic surface fitting and kriging", *Journal of Hydrology*, **195**(1-4), pp 160-171 (1997).
12. Amani, A. and Lebel, T. "Lagrangian kriging for the estimation of Sahelian rainfall at small time steps", *Journal of Hydrology*, **192**(1-4), pp 125-157 (1997).
13. Abtew, W.O. and Ahih, G. "Spatial analysis for monthly rainfall in South Florida", *Wat. Resour. Bull.*, **29**(2), pp 179-188 (1993).
14. Musavi Nejad, S.H. "Determination of the best interpolation method for arid and semiarid climates of the central basin of Iran", M.Sc. Thesis, Dept. of Education and Research, Ministry of Jihad Sazandegi, Tehran, I.R. Iran (2000).
15. International Institute for Aerospace Survey and Earth Sciences, Integrated Land and Water Information System (ILWIS), *Remote Sensing & GIS Software Package*, The Netherlands (1998).
16. Petkov, L., Pieri, M., Maselli, F. and Maracchi, G. "Study and modeling of temperature spatial variability by NOAA-AVHRR thermal imagery", *ISPRS Journal of Photogrammetry and Remote Sensing*, **51**(3), pp 127-136 (1996).
17. Thiessen, A.H. "Precipitation avarages for large areas", *Monthly Weather Rev.*, **39**(7), pp 1082-1084 (1911).
18. Watson, D.F. and Philip, G.M. "A refinement of inverse distance: Weighted interpolation", *Geo-Processing*, **2**, pp 315-327 (1985).
19. Seaman, R.S. "Objective analysis accuracies of statistical interpolation and successive correction schemes", *Aust. Meteo. Mag.*, **31**, pp 225-240 (1983).